ARTICLE IN PRESS

Demand management with limited cooperation among travellers: A doubly dynamic approach☆

Mehmet Yildirimoglu [a,*], Mohsen Ramezani [b]

[a] *The University of Queensland, School of Civil Engineering, Brisbane QLD 4072, Australia*
[b] *The University of Sydney, School of Civil Engineering, Sydney NSW 2006, Australia*

ARTICLE INFO

ABSTRACT

This paper proposes a demand management method that optimizes the network performance by manipulating departure times within limited cooperation settings. The framework builds on the restricted flexibility of travellers' departure times and exposes the impact of minimal changes in travellers' schedule on the overall network performance. The test-bed (the plant) is based on the trip-based Macroscopic Fundamental Diagram (MFD) that relates the network space-mean speed to the vehicle accumulation. Travellers in the trip-based MFD model are characterized by their specific desired arrival times, heterogeneous trip lengths, and earliness and lateness scheduling penalties. The optimization problem, on the other hand, is formulated based on the accumulation-based MFD model that relates the network production (i.e. length-weighted aggregated link flows) to the vehicle accumulation. The accumulation-based MFD is an aggregated parsimonious model and does not consider individual traveller attributes, which enables it to remain analytically tractable and makes it suitable for optimization purposes. The proposed demand management method is also incorporated into a day-to-day evolution model where travellers adapt based on their historical departure times, experienced travel costs, and individual characteristics. The results highlight that the accumulation-based MFD can be efficiently used to develop travel demand management methods with realistic representation of traffic congestion within and across days.

© 2019 Elsevier Ltd. All rights reserved.

1. Introduction

The equilibrium analysis in transportation networks has received extensive attention in the literature and has laid the foundation for considerable applications in transportation planning and management. Specifically, departure time analysis has been traditionally studied in the morning commute context from a Vickrey equilibrium perspective (Vickrey, 1969). Vickrey considers point bottleneck models with constant capacity (i.e. fixed outflow under congested conditions) and defines equilibrium distribution of arrival times at the bottleneck over a morning peak period. In this framework, a traveller experiences an actual delay (due to waiting in the queue) and a schedule delay (due to earliness or lateness). While all travellers adjust their departure times to minimize their individual travel costs, equilibrium is reached when no traveller

has an incentive to change their departure time. Vickrey's model has been extended to analyze existence and uniqueness of Nash equilibrium (Smith, 1984; Daganzo, 1985), consider heterogeneous travellers (Newell, 1987), and develop optimum toll strategies (Arnott et al., 1990). Although the focus in Vickrey's equilibrium is point bottlenecks, the theory has been applied at the network level too (Small and Chu, 2003; Geroliminis and Levinson, 2009). Nevertheless, FIFO assumption is fundamental to the analytical Vickrey model, and heterogeneous trip lengths that travellers might have in a network setting requires a careful investigation of its large-scale impacts (Daganzo and Lehe, 2015; Fosgerau, 2015; Liu and Geroliminis, 2016; Lamotte and Geroliminis, 2018).

Transportation networks exhibit intra-day (within-day) and inter-day (day to day) fluctuations in traffic states, due to the highly-correlated, chaotic, and intricate dynamics of traffic and travellers' decision making (departure time choice, route choice, etc.). This raises the interest to scrutinize day-to-day models of transportation networks (e.g., Bie and Lo, 2010; Cantarella et al., 2015; Xiao et al., 2016; Xiao and Lo, 2016; Liu and Geroliminis, 2017 and others). The day-to-day modeling framework can be utilized to devise and evaluate congestion control strategies (e.g., Guo et al., 2015), pricing schemes (e.g., Tan et al., 2015), and demand management methods, such as this paper, to investigate the medium- and long-term effects of travel optimization measures on transportation networks. Day-to-day models can also be integrated with models of within-day traffic dynamics to capture the temporal propagation of congestion in the network during the day, i.e. doubly dynamic models.

The analytical models that rely on Vickrey equilibrium have focused on idealized cases and generated significant insights onto the fundamental principles that should govern traffic planning and management systems. Although the problem becomes cumbersome due to observability issues in wished arrival times, heterogeneity across travellers, tediousness of the analytical approach and fundamental assumptions underlying the traffic flow modeling, the findings from these studies lay the foundation and produce the guidelines for effective planning and management schemes. Nevertheless, this paper investigates the problem from a control perspective. Therefore, the type of outcome/conclusions is different in nature from the existing studies, as it focuses more on benefits from a management (or control) strategy, rather than insights for potential applications. This paper aims at developing a novel travel demand management method that captures the (limited) flexibility of departure time choice and exploits the potential benefit from the cooperation of users across time (e.g., non-peak usage, flattening peak demand). The proposed travel demand management scheme manipulates the departure time of travellers in a large-scale network and accounts for travellers' reaction and adaptation through a day-to-day evolution model. Emerging communication technologies will allow transportation authorities to easily interact with the users and intervene with their travel decisions. It is, therefore, a timely effort to reformulate the departure time choice phenomenon as a central optimal control problem. Macroscopic Fundamental Diagram (MFD) is adopted to maximize the system performance by rescheduling travel demand and be integrated with a day-to-day model as a large-scale network modeling tool. MFD provides a unimodal, low-scatter and demand-insensitive relationship between network-wide traffic states (e.g. accumulation, speed, production, and trip completion flow) for an urban region.

The concept of MFD with an optimum accumulation is initiated by Godfrey (1969). Similar ideas are later introduced by Herman and Prigogine (1979), Mahmassani et al. (1984), Daganzo (2007), while the empirical existence of MFD is shown by Geroliminis and Daganzo (2008). Despite having shortcomings related to heterogeneity (i.e., the region should have low heterogeneity for a well-defined MFD to exist) and hysteresis (MFD may behave differently on the onset and offset of congestion), MFD is a powerful modeling tool that enables the development of parsimonious and tractable dynamical models for large-scale urban road networks. This modeling approach has offered the possibility of designing network-level traffic management and control schemes. Some examples are perimeter control in urban networks (Geroliminis et al., 2013; Keyvan-Ekbatani et al., 2015; Ramezani et al., 2015; Kouvelas et al., 2017; Yang et al., 2018; Aalipour et al., 2018), regional route guidance (Yildirimoglu et al., 2015; Sirmatel and Geroliminis, 2017; Yildirimoglu et al., 2018), pricing (Zheng et al., 2016; Gu et al., 2018), and control of city-scale ride-sourcing systems (Ramezani and Nourinejad, 2018). Further studies on the properties of aggregated network modeling using MFD (e.g. Gonzales and Daganzo, 2012; Mahmassani et al., 2013; Laval and Castrillón, 2015; Ambühl and Menendez, 2016; Laval et al., 2018; Amirgholy and Gao, 2017; Amirgholy et al., 2017) herald the progress towards a new generation of network-level traffic modeling and control schemes.

The (traditional) MFD modeling builds a relation between the network production (i.e. length-weighted average link flows) and the accumulation of vehicles. It does not consider individual vehicle attributes or driver decisions, and builds upon an average vehicle trip length that casts speculations about the level of consistency, particularly for open-loop modeling purposes (Yildirimoglu and Geroliminis, 2014; Leclercq et al., 2015). We refer to this model as the accumulation-based MFD model. Recently, a few studies (e.g. Arnott, 2013; Mariotte et al., 2017; Lamotte and Geroliminis, 2018) explored 'trip-based' MFD reformulation to address the effect of variable trip lengths on dynamics of congestion in single-reservoir networks. The trip-based MFD model tracks the travelled distance of all vehicles by assuming that a well-defined relationship exists between network accumulation and average speed.

This paper incorporates the two realistic representations of city-scale traffic dynamics, i.e. accumulation- and trip-based MFD models into a day-to-day model to develop a novel travel demand management strategy. The accumulation-based MFD model is embedded in the optimization problem to maximize the network performance without the need to acquire characteristics of individual travellers such as wished arrival times, trip lengths, and scheduling penalties. In the day-to-day framework, the optimized departure times are allocated to travellers and evaluated by the trip-based MFD model that is capable of considering the detailed characteristics of individual travellers. This framework allows us to simultaneously utilize the tractability of parsimonious accumulation-based MFD for optimization purposes and detailed features of the
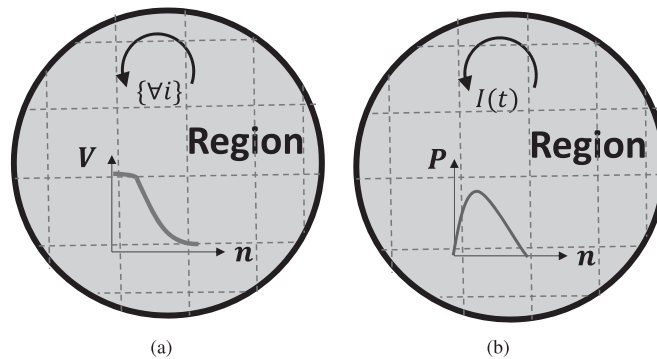
Fig. 1. Network structure: (a) Trip-based MFD model representation and (b) Accumulation-based MFD model representation.

trip-based MFD to provide a more-detailed representation of traffic dynamics. The results demonstrate promising outcomes to reduce total travel time spent in the network and highlight the advantages of MFD modeling.

The contributions of this paper are multi-fold. (1) We develop a demand management strategy that relies on limited changes in departure times and analytical tractability of the accumulation-based MFD model. While MFD models have been exploited to develop various management schemes, the aspect of cooperation in departure time choice has not been investigated before. (2) We explore the model-plant mismatch using the accumulation-based and trip-based models. Note that these two models are inherently different in the way they model the congestion dynamics. (3) We integrate a day-to-day evolution model with the trip-based MFD model and explore the medium term impacts of the proposed disruptive travel demand management strategy.

The remainder of this paper is structured as follows. In Section 2, we elaborate the main modeling assumptions of the day-to-day learning procedure and departure time optimization method, and present the traffic flow models. In Section 3, we present the overall integrated framework that consists of the day-to-day model and the demand management method. Finally, in Section 4, we assess the proposed day-to-day and demand management model using numerical experiments and analyze the properties of equilibrium solutions. Section 5 concludes the paper and outlines future research directions.

2. Modeling preliminaries

2.1. Modeling assumptions on network, decision mechanism, and control

Assumption 1. We consider a single-region city, where the origins and destinations of travellers are located within the region, see Fig. 1. We assume there is no demand from the periphery of the city. Nevertheless, this assumption can easily be relaxed in future works to allow a multi-reservoir network representation.

Assumption 2. We employ two models that possess distinct features but are based on the same aggregated performance function (i.e. MFD). The trip-based MFD model is used as the plant that is capable of modeling the departure time choice of individual travellers (i) considering disaggregated desired arrival times, trip lengths, and schedule penalty costs. The trip-based MFD model assumes the average speed of the region (V) is a function of region accumulation (n), see Fig. 1(a). The parsimonious accumulation-based MFD is used for departure time optimization to keep the problem tractable. It does not require detailed information from each traveller. This model keeps track of region accumulation based on the total production of the region (P), which is a function of accumulation (n), and aggregated inflow to the region (I), see Fig. 1(b). Using the two different yet consistent models (note that $V = P/n$) in the travel demand management method highlights the potential of aggregated network-scale models for congestion management.

Assumption 3. Each traveller (or agent) has her/his own desired arrival time (to her/his destination), trip length, and earliness/lateness cost (or penalty) coefficient.

The trip-based MFD model, which is described in Section 2.3, allows us to build a disaggregated, detailed and yet city-scale model where travellers make departure time decisions with respect to their own desired arrival time and schedule cost perceptions. Although in reality the travellers might update/change their routes within and across days in response to the changing traffic conditions, in this work, we assume the trip distance is a constant value and does not depend on traffic. Future work might relax this assumption considering a link-level representation of the traffic network and a route assignment model that considers alternative paths between origin and destination of travellers.

Assumption 4. The travellers' decision making only involves the departure time choice over days. The route choice, origin / destination choices, mode choice and no travel option are not considered. Note that this assumption can be interpreted such that the mode choice is done a priori where multiple modes are available in the network. In addition, the passenger

occupancy of each vehicle is considered one; every one travels alone. This implies that the total car demand over days (iterations) is fixed and also their trip lengths do not change.

Assumption 5. Travellers adapt their departure time choice to minimize their total travel cost (travel time plus the scheduling penalty). Travellers do not shift their departure times by more than τ [unit of time] in a day with respect to their previous departure time.

This assumption reflects the myopic capability of the travellers in perceiving the travel costs and changing their departure time decisions. Generally, it is expected that the travellers have inertia to drastic changes in their departure time choice and have tendency towards experimenting alternatives in the vicinity of their previous day choice.

Assumption 6. In the day-to-day model, in addition to the travel cost they experience at the chosen (or allocated) departure time, we assume travellers know the real-time instantaneous travel time (from, e.g., traveller information systems) for the other (potential) departure times (in vicinity of their actual departure time $\pm \tau$) at the end of each day. To the best of our knowledge, most commercial traffic information apps provide instantaneous travel time information which is solely based on current traffic conditions or historical travel times. Although there exists a certain level of inconsistency between the instantaneous and experienced travel times (see Yildirimoglu and Geroliminis, 2013), we assume travellers can account for that using the correction mechanism presented in the day-to-day evolution model (described more in detail in Section 3.2).

Assumption 7. The average trip length is assumed to be known from the demand management (or traffic control) perspective.

While the travellers have heterogeneous trip lengths in the network, we assume an accurate estimate of the average trip length across all the travellers is available. In reality, the trip length of the travellers can be monitored with data from probe vehicles, Bluetooth sensors, etc., and an accurate average value can be estimated even with low penetration rates.

Assumption 8. An online platform (e.g., a website, a smart phone app) is introduced to establish the communication between the travellers and the central controller (i.e., demand management model). Travellers request departure times and are allocated new departure times via this platform. From the perspective of the demand management system, we assume the requested departure times are given and the allocated departures time can be communicated back to the travellers.

2.2. Accumulation-based MFD model

The accumulation-based MFD model serves as the optimization model that the travel demand management strategy (i.e. departure time optimization) is built on, while the trip-based MFD model serves as the plant (i.e. reality), which represents the test bed. These two models rely on equivalent representations of the MFD function, but have inherently different approaches to model traffic congestion dynamics. The accumulation-based MFD model considers 'production-MFD', $P(n)$, as a function of accumulation, n, (i.e. the number of vehicles circulating in the network) and models the traffic dynamics through tracking the temporal evolution of accumulation as

$$\dot{n}(t) = I(t) - O(n(t)) \tag{1}$$

where $n(t)$ is the accumulation at time t, $\dot{n}(t)$ is the derivative of accumulation with respect to time, $I(t)$ is the inflow rate to the region and $O(n(t))$ is the vehicles outflow rate at time t. Considering a constant average trip length, $\bar{l}$, and assuming slow-varying demands the outflow can be estimated as $O(n(t)) = P(n(t))/\bar{l}$, see Assumption 7.

Due to its low complexity and analytical tractability, accumulation-based model is a promising tool to develop network-level traffic management schemes. However, under rapidly changing traffic conditions, it might not provide a good approximation as it produces inconsistent lag in information propagation. For instance, a sharp increase in the inflow rate results in an immediate increase in the outflow rate (i.e. information propagation at infinite speed). Nevertheless, in reality, outflow should increase only when the new vehicles reach their destinations or the region boundary. This is a well-known defect of outflow models (Mun, 2007). To account for the aforementioned information lag or the reaction time, a possible solution is to augment the accumulation-based MFD model with the state delay in the MFD output (Haddad and Zheng, 2018). Another approach, studied in Daganzo and Lehe (2015), Lamotte and Geroliminis (2018), Mariotte et al. (2017) is a new formulation where all vehicles might have variable trip lengths and move toward their destination with respect to the average speed in the region defined by "speed-MFD", $V(n)$. This function can be expressed as $V(n) = P(n)/n$, and it provides an equivalent representation to the production-MFD.

2.3. Trip-based MFD model

The trip-based MFD model (as presented in Mariotte et al., 2017; Lamotte and Geroliminis, 2018) is a discrete event-based simulation model that is capable of treating individual vehicles based on their departure times (from the origins) and trip lengths. The events consist of departure and arrival (at destination) of vehicles in the network. The trip-based model considers the region speed $V(n(t))$ and calculates the remaining trip distance of circulating vehicles until the next event occurs, i.e. either a new vehicle is generated in the network or a vehicle reaches its destination. In the former situation, the number of vehicles in the region increases by one and region speed drops accordingly, because $dV/dn < 0$. In the latter situation, the number of vehicles in the region decreases by one and the region speed increases accordingly. Once a vehicle

traverses its entire trip distance, its arrival time at the destination is recorded. This leads to determination of the travel time and scheduling cost of individual traveller. The fundamental relation between the trip length of traveller i, l_i, the departure time of traveller i, t_i^{dep}, and network speed, $V(.)$ is:

$$l_i = \int_{t_i^{\mathrm{dep}}}^{t_i^{\mathrm{dep}} + T_i^{\mathrm{exp}}(t_i^{\mathrm{dep}})} V(n(t)) \, \mathrm{d}t \tag{2}$$

where $T_i^{\mathrm{exp}}(t_i^{\mathrm{dep}})$ denotes the experienced travel time of traveller i in the network departing at time t_i^{dep}.

The trip-based MFD model serves two purposes: (i) to establish the day-to-day equilibrium conditions without any demand management action and (ii) to evaluate the effect of the demand management strategy at day d and to model the change in departure time choice of passengers. The use of the trip-based MFD model as the test bed, item (ii), allows us to capture the model-plant mismatch that is inevitable in any control application. This is due to the distinct features of the trip-based and the accumulation-based MFD models. Note that any other traffic model (e.g. microsimulation) that potentially offers an accurate representation of the congestion dynamics of the system and serves the two above purposes in a tractable manner can be used in the proposed demand management strategy. It is worth mentioning that that number of travellers is a key factor in the computation complexity of the trip-based MFD model. In contrast, the computation complexity of the accumulation-based MFD model is not a function of the number of travellers, which highlights the main advantage of using the accumulation-based MFD model for the optimization. The pseudo code of the trip-based MFD model reads as:

Algorithm 1 Trip-based MFD pseudo-code.

Initialize each traveller (i): $\{t_i^{\mathrm{dep}}, T_i^{\mathrm{w}}, l_i,$ scheduling penalties$\}$
Initialize event_list = [ ]
Initialize output = [ ]
Initialize $n = 0$ %vehicle accumulation
Initialize $j = 0$ %event counter
Initialize $t_j = t_{\mathrm{init}}$

current_speed = $V(n)$
for All vehicles (i) **do**
    event_list $\leftarrow t_i^{\mathrm{dep}}$, that is the initial requested departure time
    Determine the potential arrival time of vehicle i, i.e. t_i^{arr}, using Eq. (2) considering constant current_speed
    event_list $\leftarrow t_i^{\mathrm{arr}}$, that is the initial arrival time
end for

Sort event_list

while Items in event_list **do**
    $j \leftarrow j + 1$
    Determine the next event closest to t_{j-1} and let its corresponding time as t_j
    $l_i \leftarrow l_i - V(n) \cdot (t_j - t_{j-1}) \quad \forall i$ %all vehicles travel a unique distance based on the network average speed and
                                       the time between events j and $j - 1$
    if The first closest event is a vehicle departure **then**
        $n \leftarrow n + 1$
    else
        $n \leftarrow n - 1$
        output $\leftarrow T_i^{\mathrm{exp}}$, i.e. the experienced travel time of vehicle i
    end if
    Remove the first closest event from the event_list
    current_speed = $V(n)$
    Update the potential arrival time of all vehicles in event_list using Eq. (2) considering new constant current_speed
end while

Note that the trip-based MFD model is not necessarily a first in first out (FIFO) model since the trip length of individual vehicles might differ.

3. Day-to-day dynamics and departure time optimization

In this section, we first present the overall framework that consists of the day-to-day model and the demand management method. Subsequently, we describe the decision mechanism of the travellers in the day-to-day evolution model and
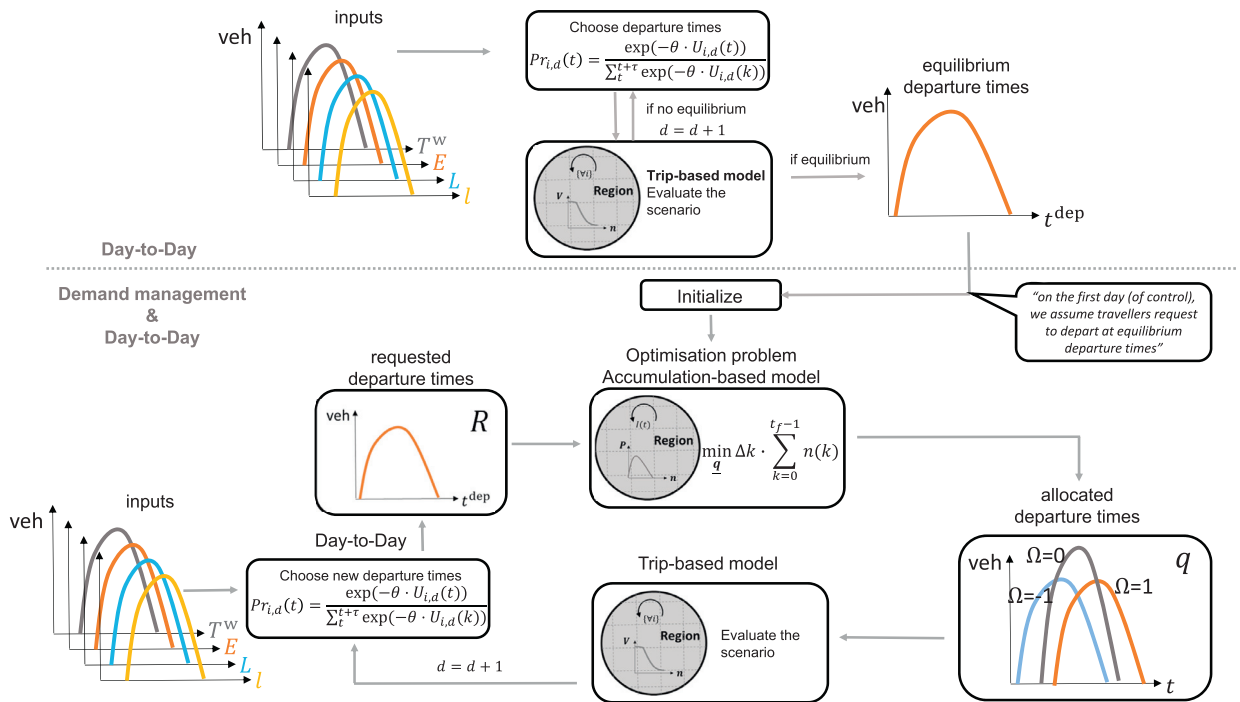
Fig. 2. Structure of the proposed departure time optimization and day-to-day learning framework.

their associated learning process with respect to the departure time choice. Finally, we present the demand management method that optimizes the network performance given the travellers' departure time request and the constraints associated with the possible changes.

3.1. The overall framework

Fig. 2 summarizes the proposed framework that includes the two MFD models, the equilibrium analysis of the day-to-day evolution model and the demand management strategy. In Section 3.2, we elaborate the day-to-day evolution of the doubly (day-to-day plus the within day) dynamics of the urban vehicular transport system (see the upper part of Fig. 2). Traveller i has his/her own desired arrival time, trip length, earliness and lateness penalties (respectively T_i^w, l_i, E_i, and L_i). Using the learning mechanism presented in Section 3.2, travellers update their departure time choice every day, and the resulting new scenario is evaluated with the trip-based model. We update the evolution mechanism until the doubly dynamical system reaches an equilibrium point where traveller decisions, travel costs and traffic conditions do not change significantly across days. Eventually, the day-to-day evolution mechanism converges to stable patterns and produces the equilibrium departure times, which are then taken to the demand management method.

In the second part of the framework, we apply the demand management method and the day-to-day learning mechanism sequentially and explore the medium-term impacts of the disruptive travel demand management strategy. On the first day when the departure time management strategy is introduced, we assume travellers request to depart at their equilibrium departure times that are obtained based on the day-to-day mechanism explained in the upper part of Fig. 2. The optimization problem presented in Section 3.3 allocates new optimal departure time periods while ensuring travellers' flexibility constraints are not violated. The trip-based MFD model, then, evaluates the newly allocated departure times and produces the new generalized travel costs for travellers. On the following day, travellers choose and request a new departure time interval based on the perceived costs of alternatives, which results in a new requested demand profile. Finally, we allocate new departure times with respect to the requested demand values and complete the loop for a day. This procedure is repeated for a certain number of days. Whether the system reaches equilibrium or not with the travel demand management strategy will be discussed in Section 4.

3.2. Day-to-day dynamics of departure time choice

Consider a discrete day-to-day departure time evolution model where days are denoted as d and the discretization step, without loss of generality, is $\Delta d = 1$. Travellers make a departure time choice on each day considering the costs they perceive for a set of departure time alternatives. Each traveller i, with a distinct wished (also interchangeably used as desired) arrival time, T_i^w, and trip length l_i, makes a departure time choice, i.e. t, based on her/his perceived (generalized) travel cost. Travellers' perception of travel costs are updated every day using the historical perceived cost and the cost they experience

or estimate on the previous day. While the experienced cost at the chosen departure time (or allocated departure time in case of the demand management scenario) is readily accessible, the cost at the other (potential) departure times can only be estimated to a certain extent. In this study, we assume that travellers can observe the real-time (instantaneous) traffic conditions through traveller information systems (Assumption 9 in Section 2.1) and estimate the travel time associated with other potential departure times through a correction factor, which will be elaborated later in this section.

Let $C_{i,d}^{p}(t)$ denote the perceived generalized travel cost for traveller i on day d with departure time t[1], and $c_{i,d}(t)$ denote the experienced (or estimated) generalized travel cost for traveller i on day d with departure time t. The update mechanism for the perceived travel cost is as follows:

$$C_{i,d+1}^{p}(t) = \omega_i \cdot C_{i,d}^{p}(t) + (1 - \omega_i) \cdot c_{i,d}(t) \tag{3}$$

where $0 < \omega_i < 1$ is the learning parameter of traveller i that defines the weights that traveller i allocates to the perceived and experienced (or estimated) travel costs. A larger ω_i represents higher reliance on the historical perceived travel cost and less importance on the most recent experienced (or estimated) travel cost from the previous day. In the numerical experiments of this study, for the sake of simplicity, we assume ω_i is identical among all the travellers, i.e. $\omega_i = \omega \; \forall i$. This assumption can be readily relaxed.

The experienced (or estimated) travel cost for traveller i on day d departing at time t is:

$$c_{i,d}(t) = \begin{cases} T_{i,d}(t) + E_i \cdot \left(T_i^{w} - t - T_{i,d}(t)\right), & \text{if } \left(t + T_{i,d}(t)\right) < T_i^{w} \\ T_{i,d}(t) + L_i \cdot \left(t + T_{i,d}(t) - T_i^{w}\right), & \text{otherwise} \end{cases} \tag{4}$$

$$T_{i,d}(t) = \frac{T_{i,d}^{\exp}(t_{i,d}^{\mathrm{dep}})}{T_{i,d}^{\mathrm{ins}}(t_{i,d}^{\mathrm{dep}})} \cdot T_{i,d}^{\mathrm{ins}}(t) \tag{5}$$

In Eq. (4), $T_{i,d}(t)$ is the experienced (or estimated) travel time that traveler i spends (or has estimated to spend) to travel trip length l_i starting from the departure time interval t on day d, and E_i / L_i are respectively the earliness and lateness coefficients associated with traveller i.

In Eq. (5), $t_{i,d}^{\mathrm{dep}}$ represents the departure time chosen by (or allocated to) the traveller i on day d, and $T_{i,d}^{\exp}$ and $T_{i,d}^{\mathrm{ins}}$ represent respectively the corresponding experienced and instantaneous travel times. As discussed before, in this study, we assume that travellers have access to instantaneous travel times through traveller information systems and they update their perceived cost of travel using this information. However, as the discrepancy between instantaneous and experienced travel times might be misleading, we assume that travellers compare the travel time they experience with the one received from the information system (for the same departure time $t_{i,d}^{\mathrm{dep}}$) and use the relative ratio between them to estimate the travel time to be experienced at other potential departure times. The first term on the right hand side of Eq. (5) indicates the ratio of the experienced travel time to the instantaneous travel time at $t_{i,d}^{\mathrm{dep}}$ and serves as a correction factor to convert instantaneous travel time to experienced travel time at other alternative departure times. For the chosen (or allocated) departure time (i.e. $t_{i,d}^{\mathrm{dep}}$), the travel time becomes equal to the experienced travel time, i.e. $T_{i,d}(t_{i,d}^{\mathrm{dep}}) = T_{i,d}^{\exp}(t_{i,d}^{\mathrm{dep}})$. For the other alternative departure times, the correction factor enables the traveller to consider an estimated travel time. Assuming that the ratio of experienced to instantaneous travel time remains approximately the same in a limited range, Eq. (5) is expected to produce accurate estimations of experienced travel time. Note that Eqs. (3)–(5) apply to departure times $t_{i,d-1}^{\mathrm{dep}} - \tau \le t \le t_{i,d-1}^{\mathrm{dep}} + \tau$, i.e. departure time choice set. The shift from the departure time choice on the previous day is limited by the time window parameter τ, as defined in Assumption 5 in Section 2.1, and the choice set, in fact, consists of discrete values that are defined by the time step Δt. Mathematically speaking, the departure time alternatives to be considered by the traveller i is $t = \{t_{i,d-1}^{\mathrm{dep}} + m \cdot \Delta t : m \in \mathbb{Z} \quad \text{and} \quad (-\tau/\Delta t) \le m \le (\tau/\Delta t)\}$. As each traveller i is randomly assigned a (continuous) departure time value on the first day, the choice set differs from user to user; however, they all consist of discrete values as defined above. As the choice set and the associated travel costs should be calculated separately for each traveller, this does not pose an issue.

As described in Eqs. (4)–(5), the generalized travel cost includes both the travel time and the schedule cost, which both hinge on the discrepancy between the instantaneous and experienced travel times. Instantaneous travel time is simply calculated using the trip length and the average speed at the departure time of the trip, i.e. $T_i^{\mathrm{ins}}(t) = l_i/V(t)$ (we omit the day index d here), while the experienced travel time is calculated by numerically solving Eq. (2).

The travellers choose their departure times with respect to the perceived utilities of departure times. The perceived utility of traveller i on day d and departure time t is defined as:

$$U_{i,d}(t) = C_{i,d}^{p}(t) + \epsilon_i \tag{6}$$

where ϵ_i is a random term that is assumed identically and independently distributed with a Gumbel distribution whose parameters can be estimated for real applications (for the whole population or several groups of users). The probability of

---

[1] While the actual departure time in the trip-based model can take any continuous value, the departure time t is selected from a range of discrete alternatives in order to take advantage of the discrete choice models. This issue will be further elaborated within this section for the definition of the choice set (departure time alternatives).

choosing the departure time t is then as follows:

$$Pr_{i,d}(t) = \frac{\exp\left(-\theta \cdot U_{i,d}(t)\right)}{\sum_{s=t_{i-1,d}^{dep}-\tau}^{t_{i-1,d}^{dep}+\tau} \exp\left(-\theta \cdot U_{i,d}(s)\right)} \tag{7}$$

where θ is the scale factor. In order to account for the commonality and correlation between the alternatives in the discrete choice analysis, one can use C-logit (Cascetta et al., 1996) or Path Size logit (Frejinger and Bierlaire, 2007). Although travel times from the neighbouring departure intervals might be correlated too, vehicles leaving at different departure time intervals will not be using the same road sections at the same time. Hence, we ignore the commonality issue and apply the conventional logit formula to compute the probability of choosing the departure time. Note that Eq. (7) defines the probability of choosing departure times for each agent separately and not in an aggregated manner.

The proposed day-to-day evolution mechanism is expected to eventually reach an equilibrium solution where the departure time decisions do not change significantly across days. This requires the perceived costs and experienced (or estimated) costs to remain the same across the days. Therefore, the perceived cost of departure time t for traveller i at the equilibrium point, i.e. $C_{i,*}^{p}(t)$, is:

$$C_{i,*}^{p}(t) = \omega_i \cdot C_{i,*}^{p}(t) + (1 - \omega_i) \cdot c_{i,*}(t). \tag{8}$$

This is indeed a fixed point solution where the perceived travel costs are equal to the experienced costs, i.e. $C_{i,*}^{p}(t) = c_{i,*}(t)$. Eq. 8 indicates that travellers estimate or experience the same travel costs repeatedly once the system convergences to the equilibrium condition. Instantaneous and experienced travel times are by definition different and therefore lead to different utility values, which might cause inconsistency between the chosen departure time interval and the others in the choice set. Nevertheless, assuming that the experienced to instantaneous travel time ratio in Eq. (5) is an accurate estimator in smoothly varying traffic conditions and in a limited range of departure time alternatives, we expect Eq. (8) to hold. This issue will be further discussed with numerical experiments in Section 4.

3.3. Demand management method

In this subsection, we develop a constrained optimization problem that capitalizes on (limited) flexibility of travellers' departure time choices. While desired arrival times are defined by work schedules and other routine activities, departure time choice, for the morning commute, is a decision that travellers have to make every day considering both the traffic conditions (their own travel time in particular) and the schedule cost; how early or late they arrive at their destination. Given that the desired arrival times and the total travel demand remain the same, we expect the system to reach an equilibrium point where the traffic conditions and departure time decisions stay approximately stationary across the days. The optimization method builds on the assumption that travellers are willing or enforced to change their current departure time decision within a limited time window (e.g., 5 or 10 min). While the optimization formulation does not explicitly address non-compliant drivers, we test this issue at the evaluation stage (Section 4.3.) and disengage the travellers for which the demand management systems incurs significant additional cost.

The optimization mechanism relies on the ability to allocate the travellers to earlier or later time slots than their requested departure time intervals. Therefore, the problem is formulated as a one-shot open-loop optimization formulation where the optimum allocation of departure times can be found simultaneously for the whole study period. To this end, we assume travellers request a departure time before the start of the study period and the demand management method allocates them to the new departure times that are not too apart from their requested ones. This framework allows us to create a limitedly cooperative system where the social cost of selfish decisions is curbed by minor changes. In other words, the resulting configuration does not entirely correspond to social optimum that one could reach by manipulating the departure times without temporal constraints; however, it represents a different aspect of cooperation between the travellers given the flexibility constraints. Note that, as discussed before, heterogeneous travellers with distinct perception of trip delay and schedule delay is one of the bottlenecks in the implementation of optimum pricing strategies. Our study, on the other hand, does not have to address heterogeneity as it assumes that people can accommodate limited changes to their schedule. We formulate this mechanism as a nonlinear constrained optimization problem that reads as follows:

$$\text{minimize}_{\mathbf{q}} \quad \Delta k \cdot \sum_{k=0}^{t_f-1} n(k) \tag{9a}$$

$$\text{subject to} \quad \text{for } k = 0, \ldots, t_f - 1 :$$
$$n(k+1) = f(n(k), I(k)) \qquad \text{(Accumulation-based MFD dynamics)} \tag{9b}$$

$$I(k) = \sum_{m=-\Omega}^{\Omega} q(k, m) \qquad \text{(Input of Accumulation-based MFD dynamics)} \tag{9c}$$

$$R(k) = \sum_{m=-\Omega}^{\Omega} q(k+m, m) \qquad \text{(Serving total demand constraint)} \qquad (9d)$$

$$q(k, m) \geq 0 \quad m \in [-\Omega, \Omega] \qquad \text{(Decision variables non-negativity constraint)} \qquad (9e)$$

where Δk is the time step for the accumulation-based MFD model, t_f is the length of the study period, f is the time discretized model of the conservation law of the accumulation-based MFD model, as in Eq. (1), $\mathbf{q}$ is the set containing all decision variables, i.e. $q(k, m)$ for all $k = 0, \ldots, t_f - 1$ and $m \in [-\Omega, \Omega]$, Ω is the half-length of flexible time window, R is the demand profile that results from requested departure times, and I is the travel demand inflow profile that results from allocated departure times. Note that $q(k, m)$ depends on two variables, k that is the allocated departure time period, and m that is the time gap between the requested and allocated departure time steps. In other words, $q(k, m)$ is m steps early or late travellers departing at time step k. If m is negative, travellers depart earlier than their requested departure time step, and vice versa. If m is zero travellers depart at the time step they request. Additionally, vehicles are not asked to depart more than Ω steps earlier or later than their requested time. In short, Eq. (9a) is the objective function of the optimization problem, Eq. (9b) defines the model dynamics in a discretized manner, Eqs. (9c) and (9d) compute the actual inflow and requested demand rates, respectively, and Eq. (9e) guarantees non-negativity of the decision variables. Note that I is the actual inflow that enters the network and affects the traffic model through the function f, R is the requested demand that we assume is given or observed from the online platform (see Assumption 8), and I and R are indirectly connected through the decision variables q.

Eq. (9a) is the objective function that minimizes the total time spent in the network which is represented by the numerical integration of discrete accumulation values. Note that the multiplication by the time step Δk does not affect the optimum solution, as it is a constant. Eq. (9b) defines the time-varying dynamics of traffic in the accumulation-based MFD model where accumulation in the next time step, i.e. $n(k + 1)$, depends on the current accumulation, i.e. $n(k)$, and demand inflow, i.e. $I(k)$, in the current time step. A detailed description of the accumulation-based model is given in Section 2.2, and f represents the temporal discretization for the approximate solutions of the ordinary differential equation presented therein. The discretization problem is tackled with the Runge Kutta method (RK4) using a step size significantly smaller than Δk. Within each step k of the accumulation-based model, we assume the inflow rate, i.e. $I(k)$ remains constant; however, we update the accumulation value in each step of RK4 and compute the number of vehicles at the end of the time step, i.e. $n(k + 1)$.

Eq. (9c) represents the optimized demand profile or implemented inflow rate (i.e. $I(k)$) which is the sum of all vehicles departing at time step k, regardless of whether they depart early or late with respect to their requested departure time (i.e. $m \in [-\Omega, \Omega]$). Note that $q(k, m)$ represents the vehicles that are allocated to departure time k and are shifted by m steps. Eq. (9d) guarantees that the requested demand at time step k, i.e. $R(k)$, will be served within the flexible time window Ω. As $q(k, m)$ is the vehicles departing at step k with m steps shift, $k - m$ represents the departure step that is requested by the vehicles. Hence, $q(k + m, m)$ in Eq. (9d) represents the vehicles that initially request to depart at step k (because $k = k + m - m$) but are placed in step $k + m$. Eq. (9e) ensures that decision variables are non-negative. Eqs. (9b)–(9e) applies to all the time steps within the study period, i.e. $k = 0, \ldots, t_f - 1$.

The demand management method builds on the accumulation-based model which works under the assumption that traffic streams as a whole are comparable to fluid streams and aims to generate and track system-level characteristics (e.g., region accumulation, transfer flows). On the other hand, the results are evaluated with the trip-based model which requires single entity level characteristics (e.g., individual trip length, departure time). Therefore, the decision variables need to be transferred across different levels of abstraction, while not all features are represented in both models. Notably, the allocation of departure times to particular travellers requires random sampling of the users irrespective of their trip lengths, schedule cost coefficients, etc. For instance, let the optimum allocated demand $q(5, 2) = 100$ [veh] (i.e. the number of vehicles allocated to the 5th step and departing 2 steps later than their request which is the 3rd step) and requested demand $R(3) = 1000$ [veh], we randomly sample 100 [veh] out of 1000 [veh] independent of their attributes and assign them to 5th departure time period. Additionally, the accumulation-based model (in the optimization formulation) is discretized with time steps Δk, while the trip-based model (integrated with the day-to-day assignment model) can accommodate finer departure time choices (with steps Δt). Note the following requirement $\Delta t < \Delta k$. Hence, each allocated traveller needs to make a finer departure time choice within the time step k. The choice set for the traveller i allocated to time step k is then $\{t_{i,d}^{\text{dep}} + m \cdot \Delta t : m \in \mathbb{Z} \quad \text{and} \quad (k-1) \cdot \Delta k \leq t_{i,d}^{\text{dep}} + m \cdot \Delta t < k \cdot \Delta k\}$. The final departure time choice is selected from this choice set using the logit formula presented in Eq. (7).

The objective function defined in Eq. (9a) considers only the total time spent in the network and does not involve the schedule cost. While the travellers update their departure time decisions considering their generalized cost that contains both the travel time and schedule cost, from an operation perspective, we ignore the schedule cost experienced by travellers (because of observability issues) and focus solely on traffic conditions in the network. As the accumulation-based MFD model does not keep track of individual travellers entering or leaving the network, it is not possible to consider the desired arrival time of each traveller and compute the schedule cost. Unless strong FIFO assumptions are applied, the accumulation-based

MFD model does not allow an estimation of the schedule cost. Nevertheless, the analytical tractability of the model makes it possible to identify the optimum allocation of departure times that guarantees minimum total time spent in the system.

The optimization problem is a nonconvex nonlinear program (NLP), which can be efficiently solved with for instance sequential quadratic programming or interior point solvers (see Diehl et al., 2009 for details). Software implementation of the optimization scheme is done using the CasADi Andersson (2013) toolbox in MATLAB 9.0.0 (R2016a), on a 64-bit Windows PC with 3.4-GHz Intel Core i7 processor and 16-GB RAM with the NLPs solved by the interior point solver IPOPT (Wächter and Biegler, 2006).

4. Results

In this section, we present the results from the numerical case studies. First, we describe the settings of the case study. Second, we discuss the results from the day-to-day evolution model. Third, we investigate the joint impacts of the demand management strategy and the day-to-day evolution model.

4.1. Numerical settings

The numerical case study is based on a single reservoir network and two demand scenarios; moderate and high congestion. The trip-based MFD model is used as the test bed (i.e., the *plant* representing reality), whereas the accumulation-based MFD model is used in the optimization framework to control the departure times. While the travellers are subject to varying trip lengths and earliness/lateness coefficients in the trip-based MFD model, the departure time optimization model employs the accumulation-based MFD model where the average trip length is constant and earliness/lateness costs are not taken into account.

Trip-based and accumulation-based MFD models are defined with respect to continuous time representation; however, the time horizon is discretized into multiple time intervals in the day-to-day evolution and the demand management model. In the day-to-day assignment model, travellers are assumed to have access to real-time instantaneous travel times for the departure times in the vicinity of their departure time (i.e. $t_{i,d}^{\text{dep}} \pm \tau$). As such departure time choice cannot be made in the continuous context. Without loss of generality, $\Delta t = 60$ [s] is considered as departure time intervals to create the choice set, i.e. $\{t_{i,d}^{\text{dep}} - \tau \cdot \Delta t, \ t_{i,d}^{\text{dep}} - (\tau - 1) \cdot \Delta t, \ \ldots, \ t_{i,d}^{\text{dep}} + (\tau - 1) \cdot \Delta t, \ t_{i,d}^{\text{dep}} + \tau \cdot \Delta t\}$ for the following day $d + 1$. On the other hand, considering the fact that requesting and allocating departure time within short intervals is not realistic from an operation perspective, the departure time optimization model considers $\Delta k = 300$ [s] intervals.

Additionally, the length of the choice set in the day-to-day evolution model is set by $\tau = 15$; representing $15 \cdot \Delta t = 900$ [s]; the size of the flexible window in the optimization model is set by $\Omega = 2$, representing $2 \cdot \Delta k = 600$ [s] before and after the requested departure time. The scale factor θ in Eq. (7) for both demand scenarios is $5 \cdot 10^{-2}$, and the utility values are in [s]. The other major numerical settings in the trip-based and accumulation-based models are presented in Tables 1 and 2. The accumulation-based and the trip-based MFD models rely on different representations of the same MFD function; production and speed MFDs, respectively. Also note that trip length and schedule cost parameters are randomly distributed according to the distributions presented in Table 2, but the values are truncated with respect to the presented ranges not to allow unreasonable settings. It is worth mentioning that the proposed method does not require any assumption on properties of schedule cost functions. The schedule cost of travellers is not used in the accumulation-based MFD model, which is employed in the optimization problem. However, it is needed in the trip-based MFD model to evaluate the day-to-day changes in the network. The trip-based model considers non-identical travellers such that traveller i is identified by his/her own departure time, t_i^{dep}, wished arrival time, T_i^{w}, trip length, l_i, earliness parameter, E_i, and lateness parameter, L_i. Note that, the first characteristic change over days while the other four characteristics do not change.

Table 1
Accumulation-based MFD model parameters.

Accumulation-based model	Specification
Production function	$P(n) = a \cdot n^3 + b \cdot n^2 + c \cdot n$ [veh.m/s]
Parameters	$a = 9.98 \cdot 10^{-8}, \ b = -0.002, \ c = 9.78$
Parameters	$\bar{l} = 4600$ [m], $n^{\text{jam}} = 10^4$ [veh], $n^{\text{cr}} = n^{\text{jam}}/3$ [veh]

Table 2
Trip-based MFD model parameters.

Trip-based model	Specification
Speed function	$V(n) = P(n)/n$ [m/s]
Trip length	$l_i = \bar{l} + \mathcal{N}\big(0, (0.2 \cdot \bar{l})^2\big), \ l_i > 0$
Earliness & Lateness	$\begin{bmatrix} E_i \\ L_i \end{bmatrix} = \begin{bmatrix} 0.5 \\ 4 \end{bmatrix} + \mathcal{N}\left(\begin{bmatrix} 0.05^2 & 0.1^2 \\ 0.1^2 & 0.4^2 \end{bmatrix} \right)$
	$E^i \in [0.3, 0.7], \ L^i \in [2.5, 5.5]$

4.2. Day-to-day evolution model

In this section, we focus on convergence properties of the day-to-day evolution model without considering the disruptive demand management strategy, i.e., the upper part in Fig. 2. Particularly, we test the day-to-day evolution model with two demand scenarios; moderate and high congestion.

To verify the convergence of the day-to-day evolution model to an equilibrium solution, we examine the inconsistency or discrepancy between the perceived costs and the experienced costs. As discussed in Section 3.2, we expect the departure time decisions not to change significantly at the equilibrium state. This can be guaranteed by identical values of experienced and perceived costs.

Fig. 3(a) compares individual experienced costs to individual perceived costs across different days in the moderate congestion scenario where the learning parameter is $\omega=0.75$. Note that each point in Fig. 3(a) represents a single traveller with a given desired arrival time, trip length, and schedule penalties. Therefore, at the equilibrium state, the travellers are expected to experience different generalized costs. In the perfect equilibrium conditions (which are difficult to reach in numerical experiments), all the points in Fig. 3(a) must align along the identity line. Hence, the deviation from this line provides an indication regarding the equilibrium properties. We clearly see that the scattered distribution of points on days 3 and 5 gradually disappears and the system reaches an equilibrium state on day 25, where experienced and perceived costs are quite close to each other.

While Fig. 3(a) depicts the evolution of individual travel costs, Fig. 3(b) further investigates the overall convergence of the costs with different values of learning parameters (ω). To scale up from individual cost comparison to the overall population convergence measure, we consider the perceived cost vector (i.e. $\mathbf{C}_d^p$) and the experienced cost vector (i.e. $\mathbf{c}_d$) representing all travellers and compute the L1 norm of the difference between them, i.e. $||\mathbf{C}_d^p - \mathbf{c}_d||_1$, and divide it by the number of travellers $|\mathbf{c}_d|$. In the moderate congestion scenario, we see that the overall inconsistency measure sharply decreases in the first 5 days and reaches a stable value after 10 days independent of the chosen learning parameter, albeit rather slowly with $\omega=0.25$. Even when ω is small and the dependence on the new experienced costs is high, the system reaches a stable inconsistency value and an equilibrium state with the developed day-to-day evolution model. Fig. 3(b) also depicts the within-day evolution of the speed and accumulation on day 25 (the last day) with different learning parameters, see the inset figures. We clearly see that the equilibrium state is identical; the changes across the scenarios with different learning parameters are minor. Note that, as travellers do not have a perceived cost on day $d=1$, the inconsistency computation starts from day $d=2$.

To further investigate the convergence properties, we present both day-to-day and within-day changes in the network in Fig. 4 (with $\omega = 0.75$). We produce contour plots of speed and accumulation for both within-day and day-to-day evolution; *x*-axis represents the within-day horizon, *y*-axis indicates the days, and *z*-axis or the colours represent the corresponding speed or accumulation values. It is evident that in the first days, the network experiences a higher congestion, represented by higher accumulation and lower speed. Nevertheless, the network converges to a less congested state after few days and remains approximately the same until the end of the period. Note the darker yellow in the accumulation (4(a)) and lighter blue values in the speed (4(b)) as days increase.

The moderate congestion scenario presented in Figs. 3 and 4 exhibit strong convergence properties, however, we note that the accumulation in this scenario does not reach the critical accumulation value (n^{cr}) and hyper-congestion regimes. Therefore, we further increase the demand level and test a more congested scenario. Fig. 5 compares individual experienced costs with individual perceived costs across different days with $\omega = 0.75$. Interestingly, we observe that the points are further away from the identity line on day 5 than they are on day 3. This happens because the new costs that travellers experience are quite different from the perceived costs and the system is moving towards divergence rather than convergence. Nevertheless, the points get closer to the identity line after day $d = 10$, and the system reaches a quasi-equilibrium state on day 25. Although the points align along the identity line on day $d = 25$, the discrepancy between perceived and experienced costs are higher compared with the moderate congestion scenario, see day $d = 25$ in Fig. 3(a).

Fig. 5(b) presents the overall inconsistency in the system across days. Unlike the moderate congestion scenario, we are not able to reach an equilibrium state for values $\omega < 0.75$. Therefore, we present two cases where the dependence on the perceived costs is relatively high; $\omega = 0.75$ and $\omega = 0.90$. For $\omega < 0.75$, travellers place a higher value on the new departure time experiences which are highly different from their perceptions, and consequently, we observe that the system does not reach a stable solution. For $\omega = 0.75$ and $\omega = 0.90$, although the evolution of inconsistency measures is utterly different, we see that the scenarios reach approximately stable values with the increase in days. Additionally, the accumulation and speed profiles of the last day presented in Fig. 5(b) show that the resulting within-day evolution of the system with two learning parameters are close to each other, albeit not identical. Heuristic solution methods, e.g., method of successive averages, are known to suffer from convergence issues particularly in congested scenarios (Sbayti et al., 2007); therefore, it is not surprising to observe convergence issues in the day-to-day assignment framework with low ω values. While the traditional traffic equilibrium has been typically achieved through optimization problems or smoothing methods, the day-to-day assignment approach focuses on the evolution of travel choices over days and the learning model which is based on past experiences of travelers. Note that the learning model presented in this paper is a standard formulation in the day-to-day assignment studies, see e.g., Bie and Lo (2010) and Cantarella et al. (2015). The parameters in the traditional equilibrium models are purely mathematical and have no physical interpretation, whereas the day-to-day models include learning factors (i.e., ω)

(a)   (b)
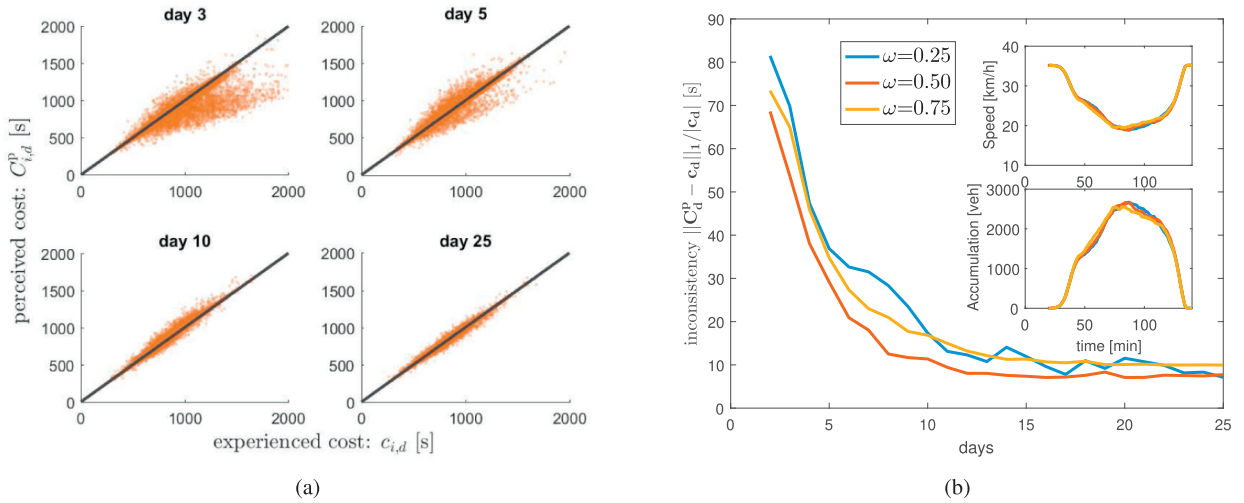
Fig. 3. Moderate congestion scenario. (a) Experienced vs. Perceived travel costs on different days with $\omega = 0.75$, (b) sensitivity of convergence to ω values and accumulation / speed profiles on the last day.

(a)   (b)
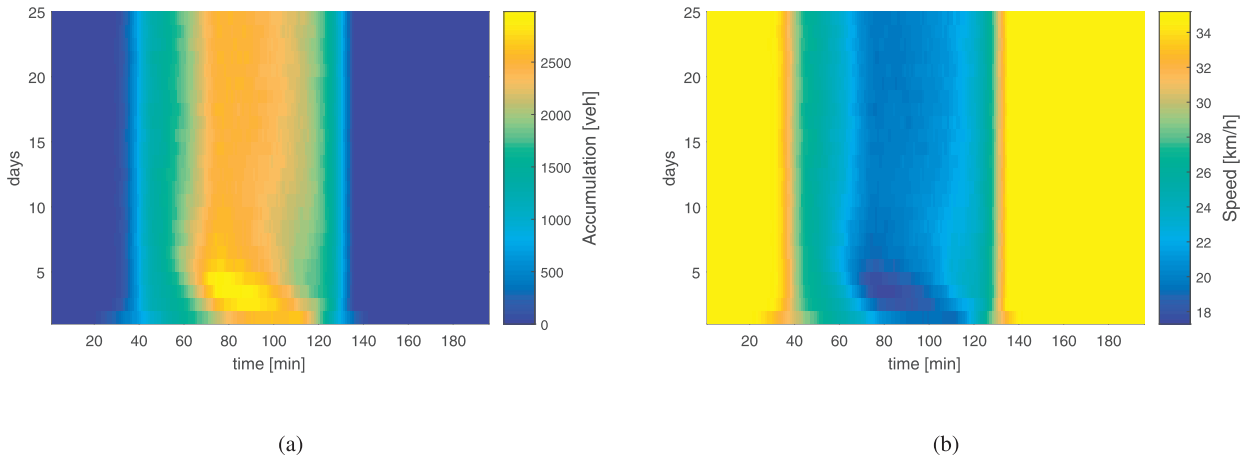
Fig. 4. Moderate congestion scenario with $\omega = 0.75$. (a) within day accumulation evolution over days, (b) within day speed evolution over days.

which in practice should be estimated with real data. A larger learning factor clearly indicates that travellers rely less on the new experience and more on the long-term experience. A large learning factor is also likely to lead to convergence, because travellers do not overreact based on single day's experience. This implies that, in congested scenarios, equilibrium can only be reached if travellers mostly rely on their historical perception.

Fig. 6 shows the day-to-day and within-day evolution of speed and accumulation values in the network with the high demand scenario and $\omega = 0.75$. The results are in line with the observations from Fig. 5. The system reaches a highly congested state between days 5 and 10, while after day 10 it reaches a relatively less congested and stable state.

4.3. Demand management method integrated with day-to-day model

In this section, we present the joint impacts of the demand management strategy and the day-to-day evolution model, as depicted in the lower part in Fig. 2. We evaluate the proposed framework using the high congestion scenario presented in the previous section. We observe similar benefits of applying the demand management model with the moderate congestion scenario, but we omit detailed discussion here to conserve space and avoid repetition. Instead, we test the high congestion scenario with and without full compliance of travellers (to the allocated departure time) and assess the robustness of the proposed method. The learning parameter is $\omega = 0.75$ throughout this section.

Fig. 7 depicts the results from the high congestion scenario with full compliance of travellers. Fig. 7(a) depicts the requested demand (i.e. $R(k)$, the aggregated demand that results from requested departure times) and the actual inflow (i.e. $I(k)$, the aggregated inflow that results from optimized departure times). Note that in this framework day $d = 0$ refers to
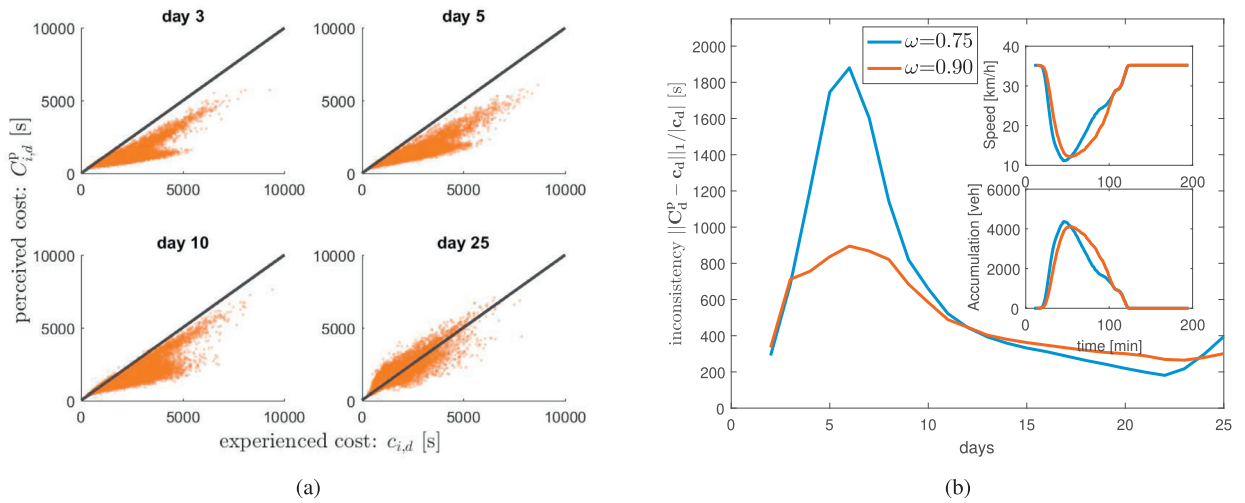
(a)

(b)

Fig. 5. High congestion scenario. (a) Experienced vs. Perceived travel costs on different days with $\omega = 0.75$, (b) sensitivity of convergence with respect to ω values and accumulation / speed profiles on the last day.
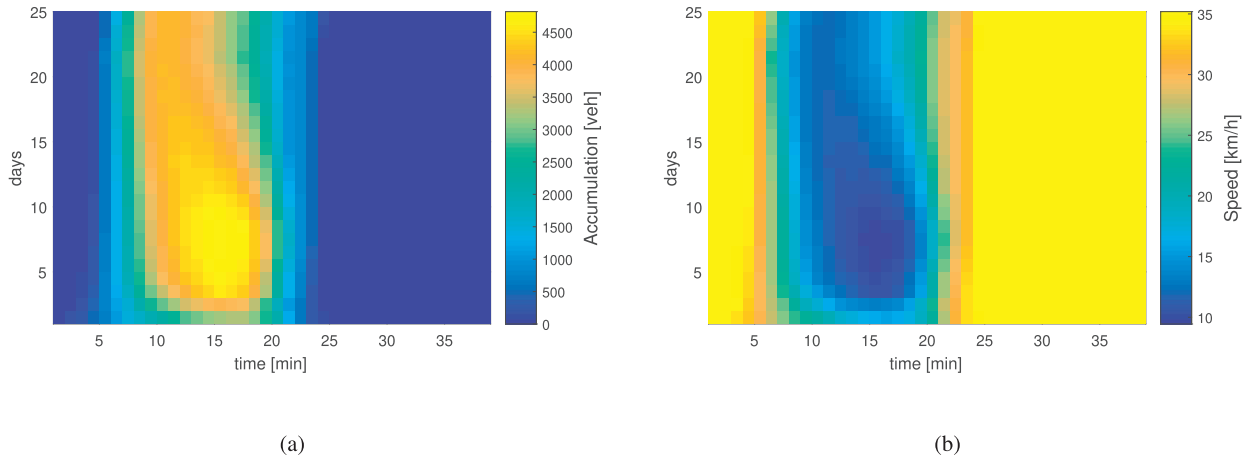

(a)

(b)

Fig. 6. High congestion scenario with $\omega = 0.75$. (a) Accumulation evolution over days, (b) speed evolution over days.

the equilibrium state from the sole implementation of the day-to-day model (see Section 3.2), day $d = 1$ is the first day the demand management strategy is applied, and so on so forth. As also presented in Fig. 2, on day $d = 1$, we assume travellers request to depart at their 'equilibrium' departure times (i.e. interval k which includes $t_{i,0}^{\text{dep}}$); the requested demand on $d = 1$ in Fig. 7(a)-inset reflects the equilibrium scenario. Starting from day $d = 2$, we notice that less travellers request to depart at earlier time intervals (see the difference between the blue curve and the others between 25 [min] and 50 [min]) and more travellers request later time periods (see the difference between 50 [min] and 100 [min]). This is due to changes in traffic conditions that are introduced by the demand management strategy. As the congestion in the network is significantly reduced (presented in Fig. 7(c)), the departure time interval that maximizes individual utility values might completely shift, which is reflected by the changes in $R(k)$. We also note that, despite minor differences between days, the overall pattern of $R(k)$ looks very much alike starting from day $d = 2$. The inflow profile $I(k)$ seems to stretch the requested demand profile $R(k)$ at both ends. The management strategy decreases the requested demand in the intermediate periods (see the difference in values of $I(k)$ and $R(k)$ between 50 [min] and 100 [min]), and creates small peaks at both ends. As the optimisation algorithm responds to the changes in $R(k)$ and the difference between days is minimal, the resulting inflow curves only have few dissimilarities across the days in the earlier time periods. We note that the inflow to the network also quickly converges to stable values in the first few days.

Fig. 7(b) depicts the decision variables of the optimisation problem (i.e. $q(k, m)$) on day $d = 30$, which represents the distribution of travellers with respect to the shift of their departure time intervals. In overall, 46% of the travellers are allocated to earlier intervals than their requested interval (i.e. $m < 0$), 47% are allocated to depart later (i.e. $m > 0$) and 7% are allowed to use their requested interval (i.e. $m = 0$).
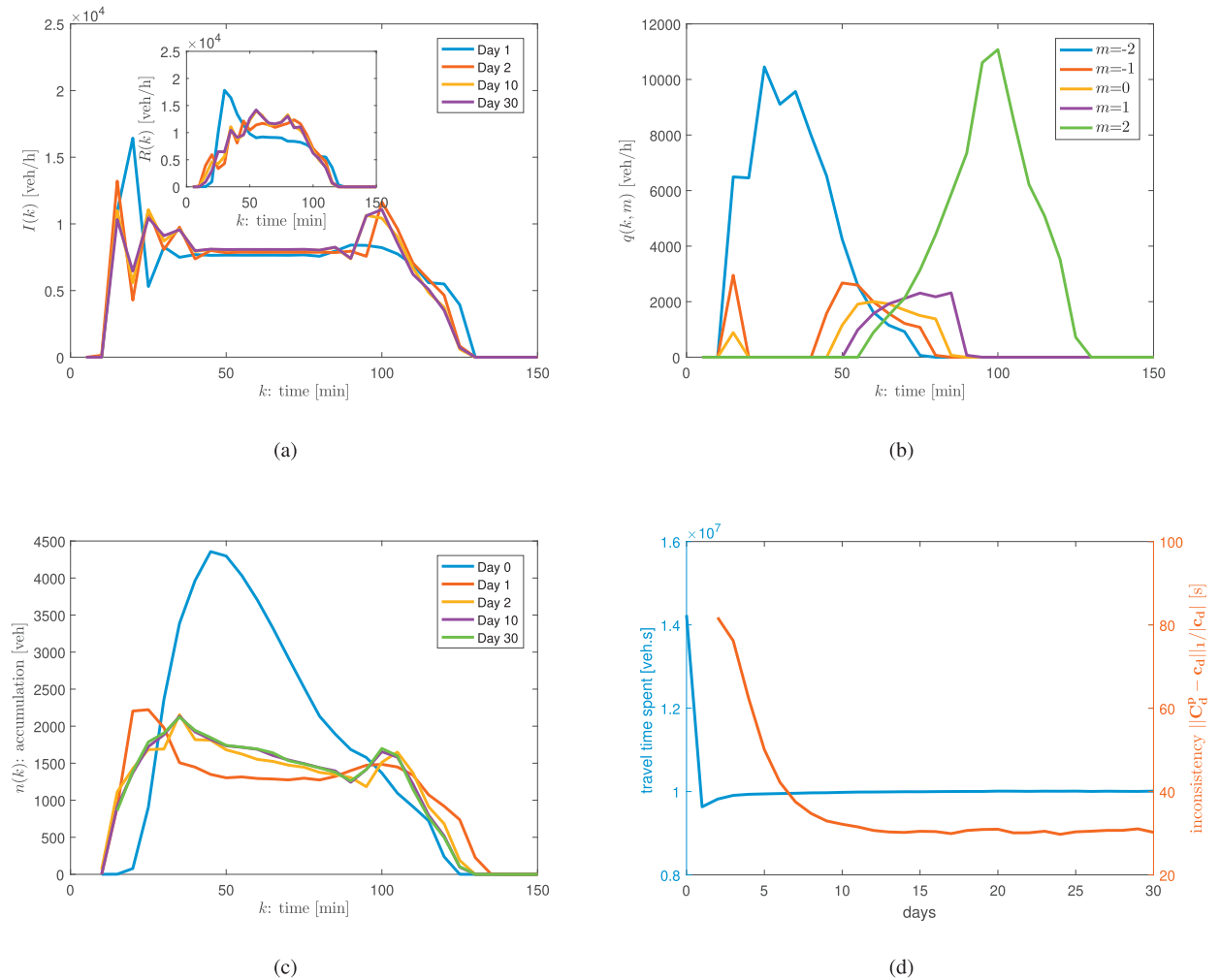
Fig. 7. High congestion scenario with $\omega = 0.75$. (a) Requested and optimized demand profiles on various days, (b) early/late demand distributions on day $d = 30$, (c) network accumulation on various days, and (d) evolution of delay and inconsistency across days.

Fig. 7(c) displays the within-day accumulation across multiple days. As clearly seen, the demand management strategy curbs the congestion and high accumulation levels starting from day $d = 1$. While the accumulation evolution is notably different on days $d = 1$ and $d = 2$, there is barely any difference between days $d = 10$ and $d = 30$. The network successfully reaches convergence day by day.

Fig. 7(d) depicts the travel time spent and the overall inconsistency measure with increasing days. We note that travel time spent in the system drops from $1.42 \cdot 10^7$ [veh.s] on day $d = 0$ to $0.96 \cdot 10^7$ [veh.s] on day $d = 1$, which is 32% drop. As the travellers adapt to the new system and make new departure time requests, the value goes up and converges to $1.00 \cdot 10^7$ [veh.s]. This is about 30% improvement in the total travel time spent. By simply shifting the departure times within 10 [min] earlier and later time intervals, we uncover the power of the limited cooperation in the traffic network. Note that the travel time spent for a vehicle consists of the delay and the free flow travel time that cannot be avoided under any circumstances. The reported benefit from the proposed strategy would be much higher if the calculation was based on the delay in the system. Fig. 7(d) also depicts the average inconsistency for travellers; i.e. the sum of inconsistency values ($||\mathbf{C}_d^p - \mathbf{c}_d||_1$ divided by the number of travellers ($|\mathbf{c}_d|$)). Surprisingly enough, we see that the inconsistency measure reaches a stable value at around day $d = 9$, while the travel time spent in the system is approximately constant starting from day $d = 2$. This implies that the aggregated patterns in the network, e.g., actual inflow, requested demand, within-day accumulation, etc., converge faster than the perceived cost of the travellers.

Even though travellers continue to make changes in their departure time choice to find their own equilibrium until day $d = 9$ (we observe this but omit detailed discussion here), the overall traffic measures converge much faster due to aggregated nature of traffic. This implies that while individual travellers switch to earlier or later time periods, the aggregated demand evolution and so traffic conditions are not affected by it.
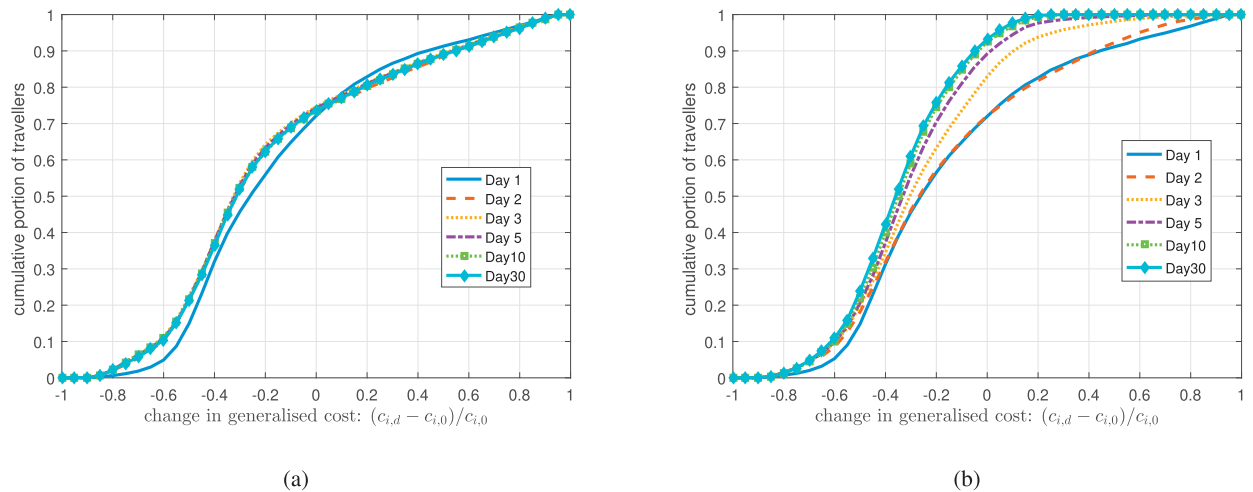
Fig. 8. Cumulative distribution of change in generalised travel cost for each individual between day $d = 0$ and others. (a) Full compliance scenario, (b) partial compliance scenario.

Note that the observations from the moderate congestion scenario (that we cannot report here due to space limitations) are complementary to the findings from the high congestion scenario. The comparison between the two scenarios shows the adaptation capability of the proposed algorithm. Briefly speaking, the changes in the desired arrival times across the scenarios lead to an equilibrium solution where the requested demand profile is distinctly different. The optimisation problem, in turn, responds to the changes in the requested demand profile and produces decision variables with distinct patterns. This confirms that the changes in R affect the patterns of the decision variables. Although the decision variables and the traffic conditions exhibit different patterns, the demand management model improves the system performance (by around 9%) and proves reliable in changing traffic conditions.

The joint implementation of the day-to-day evolution model and the demand management strategy leads the system to a new equilibrium solution, where the characteristics differ from the sole implementation of the day-to-day model. Without demand management strategy, travellers make a choice with respect to the utility of the alternative departure times and experience the cost associated with their choice. In the equilibrium solution, travellers repeatedly perceive and experience the same costs and make the same choices. On the other hand, the demand management method manipulates their choice and allocates them to a nearby interval. Therefore, in the new equilibrium solution, they repeatedly make the same choice and repeatedly get allocated to another interval which remains the same over the days. Note that even on day $d = 30$, the requested demand and the actual inflow values are distinctly different, see Fig. 7(a).

The optimization problem presented in Eq. (9) aims to minimise the total time spent in the network assuming that driver compliance is not an issue, however travellers may be reluctant to follow the control decisions when the system imposes a much larger generalized cost on them. It is therefore crucial to analyse the impact of compliance on the network performance under realistic settings. Fig. 8(a) provides the cumulative distribution of change in the generalized travel cost (normalised and compared with respect to the cost in the equilibrium scenario at $d = 0$), i.e. $(c_{i,d} - c_{i,0})/c_{i,0}$. We note that the distribution looks quite similar starting from day $d = 2$, while the first day exhibits a distinct pattern. Although around 75% of the travellers enjoy a reduction in their generalized cost, approximately 15% of the travellers suffer more than a 25% increase in their generalized cost. Assuming full compliance of these travellers might be considered unrealistic. Therefore, we relax the full compliance assumption and consider a scenario where travellers comply with the given guidance in case the suggested departure time does not impose more than 25% increase in the generalized cost. This calculation is based on perceived travel cost values; if the perceived travel cost for the suggested departure time is less than 125% of the experienced travel cost at the equilibrium, travellers comply. Otherwise, they do not comply and choose the departure time they had requested. Note that, in both full and partial compliance scenarios, the optimisation problem defined in Eq. (9) remains the same, which implies the compliance rate is not known from the controller perspective. Future work should look into estimating and incorporating these rates into the optimisation formulation. Fig. 8(b) presents the cost distributions across several days with the new compliance rules. The partial compliance scenario on day $d = 1$ is practically the same as the full compliance scenario, because we assume, on day $d = 1$, everyone wants to try out the new system regardless of the additional cost the suggested departure time might incur. From day $d = 2$ onward, the partial compliance measure is implemented. Despite the 25% cost increase threshold, we observe that many travellers experience higher travel costs (e.g., approximately 15% of the travellers experience more than 25% increase on day $d = 2$). This is due to the fact that travellers make a decision based on the cost they perceive associated with the suggested departure time; however, they might experience a largely different cost on the following day. Particularly, on the first few days where the demand management strategy is introduced, traffic conditions sharply change, which limit the perception (or the estimation) ability of the travellers. We

(a)   (b)
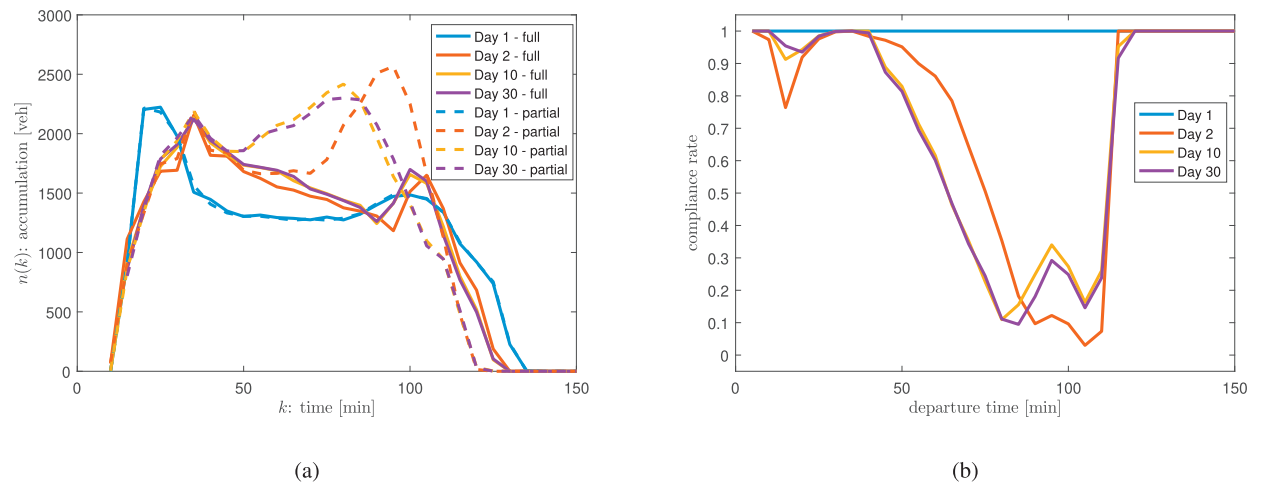
Fig. 9. (a) Accumulation values with full compliance and partial compliance scenario on several days, (b) travellers' compliance rate vs. departure time on several days.

note that the distribution shifts towards the given threshold value day-by-day; starting from day $d = 10$, we do not observe any traveler experiencing a higher cost than the given threshold value.

While the system shows convergence features even with the above compliance rules, the demand management model can prove useful only if the resulting conditions improve the network performance. Fig. 9(a) depicts the accumulation values on several days with full and partial compliance rules. As all the travellers comply with the guidance on the first day, the difference between the scenarios is only negligible (any difference is due to the randomness in the allocation of travellers). In the remaining days, we observe significantly higher accumulation values in the later time periods of the partial compliance scenario, whereas the earlier time periods do not exhibit a significant difference. We also note that the difference between day $d = 10$ and $d = 30$ is only minor, which indicates convergence in the system. Despite the significant difference in the accumulation profiles between the two compliance settings, the resulting scenario indicates a major improvement over the no control scenario. In the partial compliance scenario, travel time spent in the network is $1.06 \cdot 10^7$ [veh.s], which is equivalent to 25% reduction over the no control scenario (only 5% worse than the full compliance scenario). Fig. 9(b) depict the within-day evolution of travellers' compliance rate on the same days. The results are in line with the previous observations; compliance rate drops in the later time periods and reaches almost zero-compliance levels. Despite the low compliance issue in certain time periods, the system enjoys great benefits as indicated by the performance metrics. As the resulting system is far less congested than the no control scenario, some travellers not complying with the given guidance do not produce detrimental effects on the overall system performance, which demonstrates the robustness of the proposed strategy.

5. Conclusion

In this paper, we propose a novel demand management strategy that builds on limited cooperation of travellers in time. The proposed strategy enforces limited shifts in travellers' departure time (e.g., 10 min early or late) in a centralised and cooperative manner to minimise the total travel time spent in the network. The optimization problem is formulated based on the accumulation-based MFD model, as it provides adequate balance between accuracy and analytical tractability. The resulting optimal departure time profile is applied to the trip-based MFD model, which serves as plant in the framework. Since the trip-based MFD model is disaggregated, albeit it relies on aggregated performance functions, the trip-based model allows us to keep track of individual travellers and model their behaviour separately. Additionally, the demand management strategy is incorporated into a day-to-day evolution model in order to investigate its medium term impacts. The results demonstrate stable patterns and higher performance in the network.

A future research direction is to extend the network to multiple regions. The multi-reservoir network modeling, which requires the integration of a route choice model within the trip-based and accumulation-based MFD models, would investigate the inter-dynamics among the regions and offer deeper insights. To improve the accuracy of accumulation-based MFD model, future research should explore solutions to guarantee smooth and slow-varying optimized travel demand and traffic states. Additionally, the proposed model can be tested with a microscopic simulation model to further consider the modeling mismatch between our aggregated and low complexity model (i.e. accumulation-based MFD model) and the fine-grained state-of-the-art traffic simulation. This will also enable to scrutinize the impact of the change in travellers' trip length over days. As the demand management strategy reduces the congestion in the network, travellers are expected to switch to different routes. This phenomenon can be addressed with a route assignment model that updates the trip lengths with respect to existing traffic conditions within the day. The future work should also study the optimization problem from a reverse

perspective and compute the optimum (desired) arrival times. The resulting model could be exploited to design staggered work schedules as well for large-scale city networks.

References

Aalipour, A., Kebriaei, H., Ramezani, M., 2018. Analytical optimal solution of perimeter traffic flow control based on MFD dynamics: a Pontryagin's maximum principle approach. IEEE Trans. Intell. Transp. Syst. 1–11.

Ambühl, L., Menendez, M., 2016. Data fusion algorithm for macroscopic fundamental diagram estimation. Transp. Res. Part C Emerg. Technol. 71, 184–197.

Amirgholy, M., Gao, H.O., 2017. Modeling the dynamics of congestion in large urban networks using the macroscopic fundamental diagram: user equilibrium, system optimum, and pricing strategies. Transp. Res. Part B Methodol. 104, 215–237.

Amirgholy, M., Shahabi, M., Gao, H.O., 2017. Optimal design of sustainable transit systems in congested urban networks: a macroscopic approach. Transp. Res. Part E Logist. Transp. Rev. 103, 261–285.

Andersson, J., 2013. A general-purpose software framework for dynamic optimization. Arenberg Doctoral School, KU Leuven Ph.D. thesis. Department of Electrical Engineering (ESAT/SCD) and Optimization in Engineering Center, Kasteelpark Arenberg 10, 3001-Heverlee, Belgium.

Arnott, R., 2013. A bathtub model of downtown traffic congestion. J. Urban Econ. 76, 110–121.

Arnott, R., De Palma, A., Lindsey, R., 1990. Economics of a bottleneck. J. Urban Econ. 27 (1), 111–130.

Bie, J., Lo, H.K., 2010. Stability and attraction domains of traffic equilibria in a day-to-day dynamical system formulation. Transp. Res. Part B Methodol. 44 (1), 90–107.

Cantarella, G.E., Velonà, P., Watling, D.P., 2015. Day-to-day dynamics & equilibrium stability in a two-mode transport system with responsive bus operator strategies. Netw. Spat. Econ. 15 (3), 485–506.

Cascetta, E., Nuzzola, A., Russo, F., Vitetta, A., 1996. A modified logit route choice model overcoming path overlapping problems: specification and some calibration results for interurban networks. In: Lesort, J.B. (Ed.), Proceedings of the 13th International Symposium on Transportation and Traffic Theory. Pergamon, Oxford, pp. 697–711.

Daganzo, C.F., 1985. The uniqueness of a time-dependent equilibrium distribution of arrivals at a single bottleneck. Transp. Sci. 19 (1), 29–37.

Daganzo, C.F., 2007. Urban gridlock: macroscopic modeling and mitigation approaches. Transp. Res. Part B Methodol. 41 (1), 49–62.

Daganzo, C.F., Lehe, L.J., 2015. Distance-dependent congestion pricing for downtown zones. Transp. Res. Part B Methodol. 75, 89–99.

Diehl, M., Ferreau, H.J., Haverbeke, N., 2009. Efficient numerical methods for nonlinear MPC and moving horizon estimation. In: Nonlinear Model Predictive Control. Springer, pp. 391–417.

Fosgerau, M., 2015. Congestion in the bathtub. Econ. Transp. 4 (4), 241–255.

Frejinger, E., Bierlaire, M., 2007. Capturing correlation with subnetworks in route choice models. Transp. Res. Part B Methodol. 41 (3), 363–378.

Geroliminis, N., Daganzo, C.F., 2008. Existence of urban-scale macroscopic fundamental diagrams: some experimental findings. Transp. Res. Part B Methodol. 42 (9), 759–770.

Geroliminis, N., Haddad, J., Ramezani, M., 2013. Optimal perimeter control for two urban regions with macroscopic fundamental diagrams: a model predictive approach. IEEE Trans. Intell. Transp. Syst. 14 (1), 348–359.

Geroliminis, N., Levinson, D., 2009. Cordon pricing consistent with the physics of overcrowding. Transp. Traffic Theory 1 (1), 219–240.

Godfrey, J., 1969. The mechanism of a road network. Traffic Eng. Control 11 (7), 323–327.

Gonzales, E., Daganzo, C., 2012. Morning commute with competing modes and distributed demand: user equilibrium, system optimum, and pricing. J. Urban Econ. 46 (10), 1519–1534.

Gu, Z., Shafiei, S., Liu, Z., Saberi, M., 2018. Optimal distance-and time-dependent area-based pricing with the network fundamental diagram. Transp. Res. Part C Emerg. Technol. 95, 1–28.

Guo, R.-Y., Yang, H., Huang, H.-J., Tan, Z., 2015. Day-to-day flow dynamics and congestion control. Transp. Sci. 50 (3), 982–997.

Haddad, J., Zheng, Z., 2018. Adaptive perimeter control for multi-region accumulation-based models with state delays. Transp. Res. Part B Methodol.

Herman, R., Prigogine, I., 1979. A two-fluid approach to town traffic. Science 204 (4389), 148–151.

Keyvan-Ekbatani, M., Yildirimoglu, M., Geroliminis, N., Papageorgiou, M., 2015. Multiple concentric gating traffic control in large-scale urban networks. IEEE Trans. Intell. Transp. Syst. 16 (4), 2141–2154. doi:10.1109/TITS.2015.2399303.

Kouvelas, A., Saeedmanesh, M., Geroliminis, N., 2017. Enhancing model-based feedback perimeter control with data-driven online adaptive optimization. Transp. Res. Part B Methodol. 96, 26–45.

Lamotte, R., Geroliminis, N., 2018. The morning commute in urban areas with heterogeneous trip lengths. Transp. Res. Part B Methodol 117, 794–810.

Laval, J.A., Castrillón, F., 2015. Stochastic approximations for the macroscopic fundamental diagram of urban networks. Transp. Res. Part B Methodol 81, 904–916.

Laval, J.A., Leclercq, L., Chiabaut, N., 2018. Minimal parameter formulations of the dynamic user equilibrium using macroscopic urban models: freeway vs. city streets revisited. Transp. Res. Part B: Methodol 117, 676–686.

Leclercq, L., Parzani, C., Knoop, V.L., Amourette, J., Hoogendoorn, S.P., 2015. Macroscopic traffic dynamics with heterogeneous route patterns. Transp. Res. Part C Emerg. Technol. 59, 292–307.

Liu, W., Geroliminis, N., 2016. Modeling the morning commute for urban networks with cruising-for-parking: an MFD approach. Transp. Res. Part B Methodol. 93, 470–494.

Liu, W., Geroliminis, N., 2017. Doubly dynamics for multi-modal networks with park-and-ride and adaptive pricing. Transp. Res. Part B Methodol. 102, 162–179.

Mahmassani, H., Williams, J., Herman, R., 1984. Investigation of network-level traffic flow relationships: some simulation results. Transp. Res. Rec. 971, 121–130.

Mahmassani, H.S., Saberi, M., Zockaie, A., 2013. Urban network gridlock: theory, characteristics, and dynamics. Transp. Res. Part C Emerg. Technol. 36 (0), 480–497.

Mariotte, G., Leclercq, L., Laval, J.A., 2017. Macroscopic urban dynamics: analytical and numerical comparisons of existing models. Transp. Res. Part B Methodol. 101, 245–267.

Mun, J.-S., 2007. Traffic performance models for dynamic traffic assignment: an assessment of existing models. Transp. Rev. 27 (2), 231–249.

Newell, G.F., 1987. The morning commute for nonidentical travelers. Transp. Sci. 21 (2), 74–88.

Ramezani, M., Haddad, J., Geroliminis, N., 2015. Dynamics of heterogeneity in urban networks: aggregated traffic modeling and hierarchical control. Transp. Res. Part B Methodol. 74, 1–19.

Ramezani, M., Nourinejad, M., 2018. Dynamic modeling and control of taxi services in large-scale urban networks: a macroscopic approach. Transp. Res. Part C Emerg. Technol. 94, 203–219. ISTTT22.

Sbayti, H., Lu, C.-C., Mahmassani, H., 2007. Efficient implementation of method of successive averages in simulation-based dynamic traffic assignment models for large-scale network applications. Transp. Res. Rec. J Transp Res. Board 2029 (1), 22–30.

Sirmatel, I.I., Geroliminis, N., 2017. Economic model predictive control of large-scale urban road networks via perimeter control and regional route guidance. IEEE Trans. Intell. Transp. Syst.

Small, K.A., Chu, X., 2003. Hypercongestion. J. Transp. Econ. Policy (JTEP) 37 (3), 319–352.

Smith, M.J., 1984. The existence of a time-dependent equilibrium distribution of arrivals at a single bottleneck. Transp. Sci. 18 (4), 385–394.

Tan, Z., Yang, H., Guo, R.-Y., 2015. Dynamic congestion pricing with day-to-day flow evolution and user heterogeneity. Transp. Res. Part C Em. Technol. 61, 87–105.

Vickrey, W.S., 1969. Congestion theory and transport investment. Am. Econ. Rev. 59 (2), 251–260.

Wächter, A., Biegler, L.T., 2006. On the implementation of an interior-point filter line-search algorithm for large-scale nonlinear programming. Math. Program. 106 (1), 25–57.

Xiao, F., Yang, H., Ye, H., 2016. Physics of day-to-day network flow dynamics. Transp. Res. Part B Methodol. 86, 86–103.

Xiao, Y., Lo, H.K., 2016. Day-to-day departure time modeling under social network influence. Transp. Res. Part B Methodol. 92, 54–72.

Yang, K., Zheng, N., Menendez, M., 2018. Multi-scale perimeter control approach in a connected-vehicle environment. Transp. Res. Part C Emerg. Technol. 94, 32–49. ISTTT22.

Yildirimoglu, M., Geroliminis, N., 2013. Experienced travel time prediction for congested freeways. Transp. Res. Part B Methodol. 53, 45–63.

Yildirimoglu, M., Geroliminis, N., 2014. Approximating dynamic equilibrium conditions with macroscopic fundamental diagrams. Transp. Res. Part B Methodol. 70, 186–200.

Yildirimoglu, M., Ramezani, M., Geroliminis, N., 2015. Equilibrium analysis and route guidance in large-scale networks with MFD dynamics. Transp. Res. Part C Emerg. Technol. 59, 404–420.

Yildirimoglu, M., Sirmatel, I.I., Geroliminis, N., 2018. Hierarchical control of heterogeneous large-scale urban road networks via path assignment and regional route guidance. Transp. Res. Part B Methodol. 118, 106–123.

Zheng, N., Rérat, G., Geroliminis, N., 2016. Time-dependent area-based pricing for multimodal systems with heterogeneous users in an agent-based environment. Transp. Res. Part C Emerg. Technol. 62, 133–148.